Mechanical Systems and Signal Processing 58-59 (2015) 308–324

Contents lists available at ScienceDirect

Mechanical Systems and Signal Processing

journal homepage: www.elsevier.com/locate/ymssp

On the identification of piston slap events in internal combustion engines using tribodynamic analysis

N. Dolatabadi, S. Theodossiades *[,1], S.J. Rothberg

Wolfson School of Mechanical and Manufacturing Engineering, Loughborough University, Loughborough LE11 3TU, UK

ARTICLE INFO

Article history:
Received 15 January 2014
Received in revised form
18 November 2014
Accepted 24 November 2014
Available online 18 December 2014

Keywords:
Piston slap
Internal combustion engines
Tribology
Dynamics

ABSTRACT

Piston slap is a major source of vibration and noise in internal combustion engines. Therefore, better understanding of the conditions favouring piston slap can be beneficial for the reduction of engine Noise, Vibration and Harshness (NVH). Past research has attempted to determine the exact position of piston slap events during the engine cycle and correlate them to the engine block vibration response. Validated numerical/analytical models of the piston assembly can be very useful towards this aim, since extracting the relevant information from experimental measurements can be a tedious and complicated process.

In the present work, a coupled simulation of piston dynamics and engine tribology (tribodynamics) has been performed using quasi-static and transient numerical codes. Thus, the inertia and reaction forces developed in the piston are calculated. The occurrence of piston slap events in the engine cycle is monitored by introducing six alternative concepts: *(i) the quasi-static lateral force, (ii) the transient lateral force, (iii) the minimum film thickness occurrence, (iv) the maximum energy transfer, (v) the lubricant squeeze velocity and (vi) the piston-impact angular duration.*

The validation of the proposed methods is achieved using experimental measurements taken from a single cylinder petrol engine in laboratory conditions. The surface acceleration of the engine block is measured at the thrust- and anti-thrust side locations. The correlation between the theoretically predicted events and the measured acceleration signals has been satisfactory in determining piston slap incidents, using the aforementioned concepts. The results also exhibit good repeatability throughout the set of measurements obtained in terms of the number of events occurring and their locations during the engine cycle.

1. Introduction

The ever increasing importance of fuel efficiency, noise reduction and engine performance is forcing researchers to better understand the mechanism and effective parameters of piston dynamics. The piston assembly plays a key role in the generation of engine mechanical losses, including noise [1]. The latter is well known as piston impact (also slap) noise. In order to better study the occurrence of slap noise events, one should carefully monitor the piston's secondary motion, which

* Corresponding author.
E-mail address: S.Theodossiades@lboro.ac.uk (S. Theodossiades).
[1] Research data for this paper are available on request from Dr. Stephanos Theodossiades (S.Theodossiades@lboro.ac.uk).

http://dx.doi.org/10.1016/j.ymssp.2014.11.012
0888-3270/

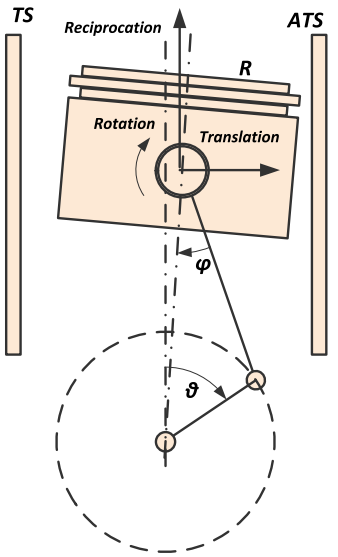

Fig. 1. Primary and secondary piston motions inside the cylinder.

leads to skirt-to-cylinder liner contacts. The excitation conditions (forces and moments) on the piston are responsible for the secondary motion, which occurs laterally within the clearance (translation) and around the piston pin (rotation). The schematic of these motions is given in Fig. 1. ϑ and ϕ are the crank and connecting rod angles, respectively [2]. R is the piston crown radius (later used to calculate the crown area). When the crankshaft rotation is clockwise, the left side of the cylinder liner is called the thrust side (TS) and the opposite side is known as the anti-thrust side (ATS). Piston impacts can occur on either side of the liner. Piston slap excites the engine block and manifests itself in the form of surface vibrations, which are eventually radiated as noise in the vicinity of the engine. In addition to the perceived benefits for engine NVH, good understanding of the number and location of piston slap events can be helpful for fuel efficiency purposes through improved system tribodynamics [2].

Previous numerical/analytical and experimental studies on piston slapping differ with regard to the way they consider lubrication effects, piston's rotation and piston skirt deformation. The common aspect in all these approaches is that they determine piston slap events (number and angular position of occurrences). In general, three approaches have been proposed in the literature to identify piston slap events based on the secondary motion of the piston. In the most simplified approach, the effects of lubrication and piston rotation are neglected. In this case, the piston's secondary motion (translation) is directly investigated using the contribution of forces in the primary direction [3–5]. This method will be referred to as *quasi-static lateral force* in this paper. Nevertheless, accurate investigation of the piston's secondary motion requires inclusion of the piston's angular motion and oil-film hydrodynamic effects. In this approach, a coupled simulation of piston dynamics and engine tribology (tribodynamics) is necessary prior to the extraction of the secondary motion [1,6,7]. Thus, the piston dynamics equations of motion are described using Lagrange's method and are coupled to the Reynolds equation for the piston skirt-liner conjunction [8]. The piston side force is extracted from the tribodynamic solution. The direction change in the side force can be used to identify the initiation of piston-slap events. Therefore, this method will be referred as *transient lateral force* in the present study. Finally, the third approach exploits the same tribodynamic analysis. In this method, the *minimum film thickness occurrence* is considered as the criterion for slap events instead of the lateral force. When the film thickness takes its minimum value (at either TS or ATS), it can be inferred that piston-liner interaction is intensified and piston slap occurs [9]. Perera et al. studied the piston-cylinder film thickness utilising the multi-physics model of a single cylinder engine. However, they considered the piston as a rigid body in their approach. The effects of friction and bearing load were included in their studies [10,11]. Three new approaches to identify piston slap events based on the tribodynamic analysis are also investigated in this study. The first approach utilises the film thickness and force variations together to calculate the transferred energy to the cylinder wall. Whenever the maximum energy is transferred, piston slap occurrence is assumed. This method will be called *maximum energy transfer*. In another approach, the rate of change in the minimum film thickness is traced to pinpoint the initiation of piston slap. As the minimum film thickness velocity changes from positive to negative, film squeeze action initiates and piston slap is assumed. This method is referred as *lubricant squeeze velocity*. The final method differs in that piston slap is indicated within a crank angular interval, whose limits are defined by the initiation of the squeeze action and the minimum film thickness occurrence methods. This interval represents the initiation and completion of piston slap. The method will be called *piston-impact angular duration*.

The six approaches chosen for investigation of the piston's secondary motion involve numerical/analytical calculations. Up to 16 potential slap events can be identified theoretically but only about 6 to 10 impacts in each cycle are observed in practice [4,12]. In order to validate the position and number of events, the experimental set-up of a single-cylinder, 4-stroke Honda petrol engine is utilised. A common practice is the attachment of accelerometers on the engine block surface. There

are different experimental set-up arrangements, depending on the measurement purposes. Chiollaz and Favre have studied noise transfer mechanisms inside the engine using several transducers [13]. Geng and Chen [4] used three accelerometers to position piston events more accurately. Richmond [14] used only one accelerometer on the engine block to capture surface vibrations. The measured acceleration contains contributions from the piston secondary motion, as well as other sources; therefore, signal processing is required to filter out the irrelevant signal content. Combustion and piston impact are difficult to separate, since their noise levels are of the same order. Moreover, they occur almost at the same time in the vicinity of the top dead centre (TDC) and are highly correlated. Pruvost et al. introduced a spectrofilter to implement the impact-source separation [15]. Geng and Chen [4] used wavelet decomposition and a fast reconstruction algorithm for this purpose. Another identification method is the blind source separation (BSS) of vibration components. The principles of this method are explained by Antoni [16]. Liu and Randall used the BSS method for the separation of internal combustion engine piston slap from other measured vibration signals [17]. Badaoui et al. [18] and Serviere et al. [19] compared Wiener filtering and BSS techniques to isolate mechanical and combustion noises. They also established a comparison between the two methods. Chen and Randall [20] have exploited the "pseudo angular acceleration" of the block to extract mechanical signals. A further study of the phase variation and frequency behaviour was applied to separate piston slap events from other mechanical sources by the same authors.

In the present study, the six aforementioned concepts will be applied in a single-cylinder engine case study for different engine speeds and loads. The surface vibration acceleration is recorded on both TS and ATS sides of the engine block. The accuracy of each method will be discussed in terms of the number and position of the mechanical events predicted, including piston slap events. The predictions are verified with experimental measurements, revealing the potential of each method for identifying piston slap events.

2. Concepts to identify piston slap events

Prior to explicitly investigating the proposed concepts, a brief description is provided about the forces and moments acting on the piston. In Fig. 2, the free body diagrams of the piston and pin are presented [7]. F_G is the gas force acting on the piston crown, F_{hyd} represents the force supported by the lubricant and F_f is the friction developed between piston and liner. m_o and m_p are piston and pin masses, I_o indicates the piston mass moment of inertia acting on piston tilt angle β about its centre of gravity. d_{COG} and d_p are the centre of gravity distance and pin offset from the piston's centre line. In the current study, pin offset is assumed to be zero and gas force F_G is assumed to act along the pin centre. As the piston reciprocates inside the liner, the connecting rod sways from side to side with its inclination introducing the force F_L at angle ϕ with respect to the cylinder axis. The inclined F_L imposes a force component, F_t, in the secondary direction. The lateral force component is given in Eq. (1). The inertial force due to gravity is considered as insignificant.

$$F_t = (m_o + m_p)\ddot{x} - F_{hyd} = F_L \sin\phi = (F_G - ((m_o + m_p)\ddot{y} + F_f sgn(y))) \tan\phi \tag{1}$$

The effect of friction force F_f on F_t is less than 2.4% and it will be neglected in this study [3]. F_{hyd} in Eq. (1) is determined using Reynolds equation, which is solved in the form of Eq. (2) [21].

$$\frac{\partial}{\partial y}\left(\frac{\rho h^3}{12\eta}\frac{\partial P}{\partial y}\right) + \frac{\partial}{\partial z}\left(\frac{\rho h^3}{12\eta}\frac{\partial P}{\partial z}\right) = \frac{\partial}{\partial y}\left(\frac{\rho h U}{2}\right) + \frac{\partial(\rho h)}{\partial t} \tag{2}$$

where, ρ, η, U, P, and h are density, viscosity, entrainment velocity, pressure and film thickness of the lubricant. The directions y and z correspond to the primary and tangential directions along the piston skirt (shown in Fig. 2).

In order to investigate the tilt action of the piston, the moments about the piston-pin are described by Eq. (3). y_{hyd} shows the distance of resultant lubricant force from pin position. a and b are the pin and centre of gravity locations with respect to

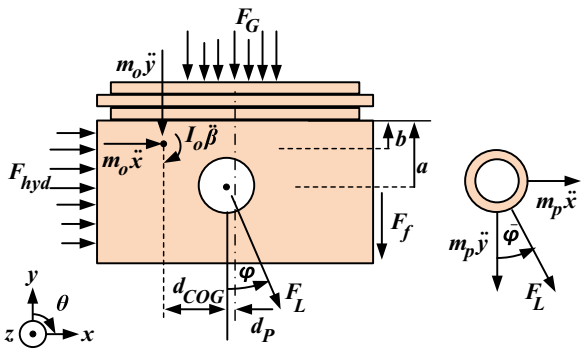

Fig. 2. Piston and pin free body diagrams.

the upper edge of piston skirt. T_f and T_G are torques due to friction and gas force about piston pin.

$$\left(I_0+m_0\left[d_{COG}^2+(a-b)^2\right]\right)\ddot{\beta}-m_o d_{COG}\ddot{y}+m_o(a-b)\ddot{x}=-T_f+T_G+F_{hyd}y_{hyd} \tag{3}$$

These three equations are the basics to the six concepts used in this study.

2.1. Quasi-static lateral force

In literature, the change of direction in lateral force is the criterion to identify piston slap [4,5]. In the first two concepts here, different methods for the identification of lateral force will be discussed. In the first concept, oil film hydrodynamic force and piston tilt are neglected. Therefore, lateral force is calculated using Eq. (1) and neglecting the F_{hyd} and friction terms. Slap events can then be directly determined using forces in the primary direction. In other words, whenever $F_G=(m_o+m_p)\ddot{y}$ or $\tan\phi=0$, piston slap may initiate. $\tan\phi$ is equal to zero at the TDC and bottom dead centre (BDC). For engines without crankshaft offset, TDC and BDC are defined at $\phi=0$ and $\vartheta=k\pi$ $(k=0,1,2,\ldots)$. When crankshaft offset is present, the $\phi=0$ positions will slightly shift in terms of crank angle. The exact ϕ value is calculated using Eq. (4). r, l and ϑ are the crank radius, connecting rod length and crank angle, respectively. C_{cs} is the crankshaft offset [22].

$$\phi=\operatorname{asin}\left(\frac{r\ \sin\ \vartheta+C_{cs}}{l}\right) \tag{4}$$

In order to determine whether piston slap occurs at TS or ATS of the cylinder liner, the value of $\tan\phi$ should be investigated along with the variations of the gas and inertia forces. Two general cases could occur within the cycle: (i) angular condition, $\tan\phi=0$ and (ii) force condition, $\sum F=0$. $\tan\phi$ has periodic behaviour. At the position where $\tan\phi=0$, if the gas force is greater than the inertia force, piston slap is expected at TS, while if the inertia force is greater than the gas force, the event happens at ATS. Alternatively, regarding the force condition, the total force can equal zero in the primary direction. This behaviour is interpreted as equality between gas and inertia forces in the graphical representation of Fig. 3. The coincidence point means that the resultant force changes direction. The sign of the force and $\tan\phi$ prior to the coincidence point can be used to identify the direction of the piston slap event. If the resultant force is greater than zero and $\tan\phi>0$, the piston moves from TS to ATS. If $\tan\phi<0$, slap occurs at TS. Providing that the force is smaller than zero prior to the incidence point and $\tan\phi>0$, then piston slides from ATS to TS. If $\tan\phi<0$, then the piston impacts the cylinder at ATS. Fig. 3 shows typical plots of the dimensionless gas force (ψ_G) and piston/pin inertia forces ($\psi_{0y}+\psi_{py}$) in the primary direction (obtained by dividing by $(m_0+m_p)r\omega^2\sin\vartheta$ to form the dimensionless contributions [5]). ω is the engine angular speed. The graph of Fig. 3 demonstrates how the method works [5]. Curves for ψ_G with higher subscript values correspond to higher engine speeds (the engine speed is increased by 1000 rpm steps for each curve). For the lowest engine speed (ψ_{G1}), the gas and inertia forces do not intersect; therefore, no piston slap is expected except at dead centres. As the engine speed increases, an incident is observed at ψ_{G2}, while at ψ_{G3} the number of incidents (slap events) increases to two. Considering the case for ψ_{G3}, there are five possible piston slap events between -180 and 180 degrees. Three of these occur at the dead centre positions. According to the method, all three events are expected at the thrust side because $F_G>(m_o+m_p)\ddot{y}$. Two incidents are observed between the gas and inertia forces at about -65 and -27 degrees. The first one happens at the ATS (with the gas force initially being higher than the inertia force and $\tan\phi$ being negative, while after the event the inertia force is higher). The second position happens at TS with the gas force being smaller than inertia forces prior to the event.

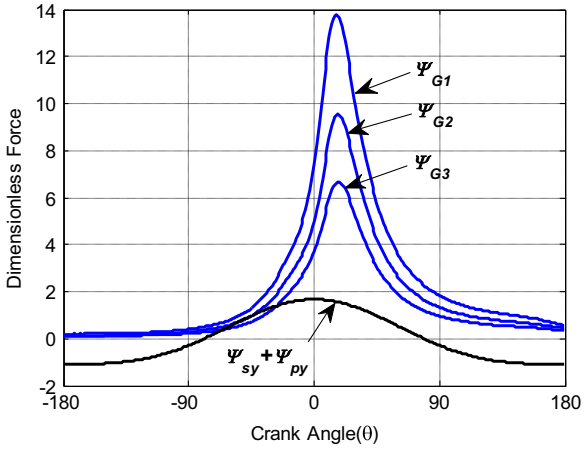

Fig. 3. Graphical representation on the use of primary forces to identify piston slaps events.

2.2. Transient lateral force

The consideration of the oil-film effect and piston rotation provides a more comprehensive description of the system's secondary dynamics. Thus, the prediction of the lateral force is achieved by solving piston dynamics with oil film tribology (solution of Eqs. (1)–(3) simultaneously). The dependency of oil density and viscosity on pressure is taken into account using Dowson-Higginson [23] and Roelands [24] expressions, respectively. The elastic deformation of the piston is considered in the film thickness expression. The elasto-hydrodynamic force is then applied on piston dynamics to calculate the lateral force as the criterion for slap events [1,9,25]. When the lateral force crosses zero and changes direction, piston slap is expected. In this approach, TS contact is indicated by negative side force values and ATS contact by positive values. Therefore, when the lateral force changes from positive to negative, piston slap is expected at TS. On the other hand, a lateral force change from negative to positive indicates events at ATS.

2.3. Elasto-hydrodynamic lubrication (EHL) minimum thickness

In this approach, the EHL minimum film thickness occurrence is the variable that identifies piston-cylinder interactions [9]. The film thickness is estimated for both TS and ATS. The solution method is similar to that of the transient lateral force criteria with the only difference being that the EHL minimum film thickness represents the exact position of piston events rather than their initiation. If the side force on the skirt is high enough to make the oil-film squeeze, then a slap event initiates. Because of the piston's tilt motion, squeeze action may take place at either side of the cylinder liner simultaneously. The side of the piston skirt, where the EHL minimum film thickness occurs, defines whether piston slap direction is towards TS or ATS.

2.4. Maximum energy transfer

Oil-film thickness and pressure are available for TS and ATS directions using piston tribodynamics. The transferred energy to the cylinder wall can be calculated between time-steps using the film properties. The product of force and oil film displacement yields the work produced. When lubricant gets squeezed, the energy is transferred to the cylinder liner. As squeeze action continues, the side force increases and work produced is expected to rise. Due to lubricant's hydrodynamic pressure, squeeze action gradually slows down. The position of the maximum work produced is assumed as that of piston slap occurrence. The direction of the event depends on whether the exploited oil properties pertain to the TS or ATS direction.

2.5. The lubricant squeeze velocity

In piston-cylinder tribodynamics, a transient solution of the Reynolds equation is obtained (the oil-film thickness and pressure depend on the oil properties, as well as its history). In Eq. (2), the term $\partial h/\partial t$ reflects oil film time history and indicates the rate of change in the film thickness. Thus, this term can be referred as lubricant squeeze velocity, which can be either negative (squeeze) or positive (separation). In order to highlight the piston slap events, the squeeze velocity is investigated for the position of the minimum film thickness. The change of sign in squeeze velocity means the squeeze action turns into separation and vice versa. The initiation of squeeze action describes piston impact; therefore, whenever squeeze velocity moves from negative towards positive values, a piston slap event is defined. The direction of the event is identified by the side of piston skirt where squeeze velocity is observed.

2.6. The piston-impact angular duration

In all previous concepts, the exact positions of piston slap events are sought. In this method, angular intervals are given to cover the entire piston impact process (from the initiation to the event completion). In order to pinpoint the positions that piston impact initiates, the lubricant squeeze velocity is exploited. The EHL minimum film thickness occurrence highlights the completion of the corresponding events. The initiation and completion positions are paired using both angular positions and directions. The angular intervals are smaller at the parts of engine cycle where greater film variations are available. The direction of the events depends on the predicted directions in the EHL minimum film thickness occurrence and the minimum film squeeze velocity criteria.

3. Experimental setup

The experimental measurements to verify the theoretical findings were made on a Honda CRF 450 R single-cylinder, four-stroke petrol engine. The engine specifications are given in Table 1. The cylinder pressure, engine speed and time-based crank angle are recorded to be used in the theoretical calculations. Surface accelerations at TS and ATS are measured by two accelerometers, which are attached to the engine block. The optical shaft encoder correlates measured acceleration with crank angle and in-cylinder pressure. The data are captured and stored using LABVIEW. The experimental setup schematic is given in Fig. 4. The gas force is calculated by multiplying the in-cylinder pressure by the piston-crown area.

4. Results and discussion

Tests were conducted for three different engine speed/load combinations: (i) 3000 rpm at 27 Nm, (ii) 3500 rpm at 40 Nm and (iii) 4250 rpm at 42 Nm. The instantaneously captured in-cylinder pressure, engine speed and crank angle are used for the tribodynamic calculations. Numerical simulations are performed for three consecutive engine cycles (at each engine speed/load combination). The number of slap events and their positions are determined for each case (and cycle). The measured surface acceleration is used for validation purposes. Since the accelerometers capture signals emitted from all engine parts, filtering and wavelet analysis have been employed to study piston events. Prior to signal processing, the expected frequency of piston slap events had to be determined. Chen and Randall [20] selected a common frequency range of 400–3200 Hz for the detection of mechanical events, including piston slap. In other papers, similar frequency intervals have been used: Ohta et al. [26] reported a frequency interval of 1–3 kHz and Nakashima et al. [27] implied the range of 500–3000 Hz. In the present study, the interval between 450 and 3500 Hz has been selected for signal processing (wavelet analysis).

4.1. Engine speed of 3000 rpm and input torque of 27 Nm

Piston secondary dynamics are initially examined for conditions of 3000 rpm engine speed and 27 Nm input torque. The calculated piston lateral force is plotted against crank angle for three consecutive engine cycles (Fig. 5). The red line shows

Table 1
Engine specification used in the experiment.

No. of cylinders	1
Fuel	Petrol
Mixing system	Carburettor
No. of strokes	4
Cooling system	Water
Bore diameter	0.096 m
Stroke length	0.0621 m
Crank shaft offset	−0.0075 m
Con-rod length	0.107 m

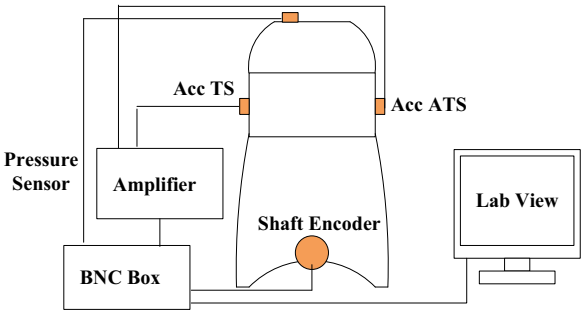

Fig. 4. Schematic of experimental set-up.

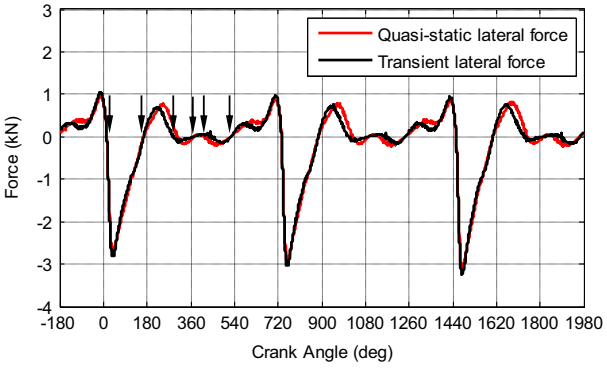

Fig. 5. Lateral force prediction (quasi-static lateral force and transient lateral force criteria) at 3000 rpm and 27 Nm.

the quasi-static lateral force due to primary forces contribution. The transient lateral force obtained from piston tribodynamics is depicted by the black line. Lateral forces reach their maxima in the combustion stroke, where the maximum gas force contribution occurs. The inertial effect of connecting rod is neglected in this study; therefore, slight deviations in the number/position of events can be expected when comparing the numerical results with the experiment. Due to crankshaft offset towards TS, the change of direction in the lateral force is expected to be delayed/advanced from the TDC/BDC by about 14°, respectively. Negative values indicate force on the TS, while positive values mean that the piston is moving in the vicinity of ATS. Using the lateral force values, six events are predicted by both criteria during a complete cycle. These are distributed across the four engine strokes, following a pattern of 0, 2, 1 and 3 events (starting at the compression stroke and ending with the intake stroke). The locations of these events are shown by black arrows in Fig. 5. Each black arrow pertains to two events (one on the red and one on the black line). The positions of these events match in the combustion stroke; however, they slightly deviate in other engine strokes where inertia forces are dominant. The positions and directions of piston slap events are given in Table 2, using the mentioned criteria.

The EHL minimum film thickness occurrence concept is examined in Fig. 6. The film thickness has been evaluated over the piston skirt surface and the minimum value is depicted (occurring at different surface locations, depending on piston deformations and tilting motion). It is assumed that the piston-liner clearance is flooded with lubricant. The black curve shows the TS minimum film thickness, while the red line corresponds to the ATS minimum film thickness. The TS film variations are smaller compared to that at the ATS. Due to crankshaft offset towards TS and the piston motion, thinner films are expected at this side. Five events are identified at each side (ten in total). The events' distribution pattern in the four engine strokes is 2, 2, 2 and 4. Red and black arrows indicate EHL minimum film thickness at ATS and TS, respectively. The exact angular positions of these arrows are given in Table 3 for each engine cycle.

The transferred energy to the cylinder wall is shown in Fig. 7. The black and red lines follow the energy behaviour at TS and ATS, respectively. As already mentioned, the maximum energy locations are assumed as piston slap events. Three large contributions can be observed in each engine cycle. The maximum energy transfer occurs through TS, in the combustion stroke. The fluctuations in the amplitude of maximum energy are due to the fluctuations in the measured in-cylinder pressure values. Ten smaller contributions exist which require closer investigation. These events are shown for the third cycle in the inset of Fig. 7. The maximum energy contributions are distributed in the engine strokes with the pattern of 3, 4, 4 and 2 events (beginning with the compression stroke). In the compression stroke, 2 events are expected at ATS and 1 event at TS. The number of events changes to 3 for TS and 1 for ATS in the combustion stroke. In the exhaust and intake strokes, 2 and 1 events occur at TS, respectively. The similar pattern of TS repeats for ATS in these strokes. In total, 13 events occur in each cycle, whose details are given in Table 4.

Table 2
Prediction of position (crank angle, degrees) and location of piston slap events for quasi-static lateral force and transient lateral force criteria at 3000 rpm and 27 Nm.

Criterion	Cycles					
	1st		2nd		3rd	
	Quasi-static	*Transient*	*Quasi-static*	*Transient*	*Quasi-static*	*Transient*
Crank angle and slap location	13 (TS)	14 (TS)	733 (TS)	734 (TS)	1453 (TS)	1454 (TS)
	166 (ATS)	166 (ATS)	886 (ATS)	886 (ATS)	1606 (ATS)	1606 (ATS)
	304 (TS)	291 (TS)	1027 (TS)	1012 (TS)	1748 (TS)	1741 (TS)
	373 (ATS)	374 (ATS)	1093 (ATS)	1093 (ATS)	1813 (ATS)	1814 (ATS)
	422 (TS)	443 (TS)	1136 (TS)	1167 (TS)	1854 (TS)	1878 (TS)
	526 (ATS)	526 (ATS)	1246 (ATS)	1246 (ATS)	1966 (ATS)	1966 (ATS)

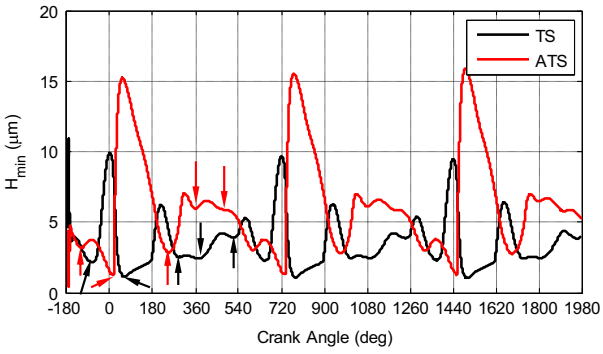

Fig. 6. The EHL minimum film thickness behaviour at 3000 rpm and 27 Nm.

Table 3
Prediction of position (crank angle, degrees) and location of piston slap events for the EHL minimum film thickness criterion at 3000 rpm and 27 Nm.

	Cycles		
	1st	**2nd**	**3rd**
Crank angle and slap location	−118 (ATS)	605 (ATS)	1322 (ATS)
	−65 (TS)	655 (TS)	1373 (TS)
	16 (ATS)	736 (ATS)	1456 (ATS)
	62 (TS)	782 (TS)	1502 (TS)
	249 (ATS)	971 (ATS)	1687 (ATS)
	292 (TS)	1015 (TS)	1721 (TS)
	363 (ATS)	1084 (ATS)	1805 (ATS)
	375 (TS)	1092 (TS)	1809 (TS)
	480 (ATS)	1203 (ATS)	1910 (ATS)
	520 (TS)	1241 (TS)	1963 (TS)

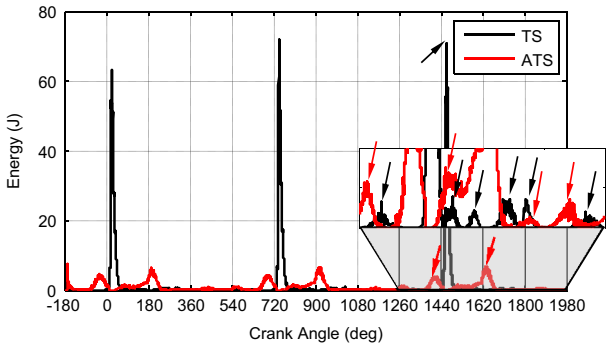

Fig. 7. The transferred energy to the cylinder wall at 3000 rpm and 27 Nm.

Table 4
Prediction of position (crank angle, degrees) and location of piston slap events for the maximum transferred energy criterion at 3000 rpm and 27 Nm.

	Cycles		
	1st	**2nd**	**3rd**
Crank angle and slap location	−154 (ATS)	563 (ATS)	1282 (ATS)
	−112 (TS)	604 (TS)	1324 (TS)
	−30 (ATS)	694 (ATS)	1418 (ATS)
	23 (TS)	745 (TS)	1465 (TS)
	78 (ATS)	805 (ATS)	1522 (ATS)
	94 (TS)	815 (TS)	1536 (TS)
	154 (TS)	876 (TS)	1596 (TS)
	192 (ATS)	915 (ATS)	1635 (ATS)
	260 (TS)	978 (TS)	1700 (TS)
	306 (TS)	1023 (TS)	1750 (TS)
	320 (ATS)	1040 (ATS)	1759 (ATS)
	442 (ATS)	1167 (ATS)	1877 (ATS)
	504 (TS)	1221 (TS)	1935 (TS)

The lubricant squeeze velocities are studied for TS and ATS in Fig. 8. The locations at which the squeeze velocity changes from positive to negative values are sought. Following this trend, 10 events are reported in each engine cycle. The events are distributed over the four engine strokes with the pattern of 2, 2, 3 and 3 events. In the first and second strokes (compression and combustion), the events are divided between TS and ATS equally. In the exhaust stroke, two events are allocated to TS, one of which also occurs at ATS. Therefore, three events are counted in this interval. Finally, one event is present at TS and two events occur at ATS in the intake stroke. Further details about the crank angles and locations are given in Table 5.

The last criterion combines the EHL minimum film thickness occurrence and the lubricant squeeze velocity. The piston impact angular durations are recorded in Table 6. According to the aforementioned procedures, the initiation of the piston slap event is estimated by the squeeze velocity. The utmost location for piston slap event to be completed is determined by the EHL minimum film thickness occurrence. The events are paired based on their timing and slap location. The last interval

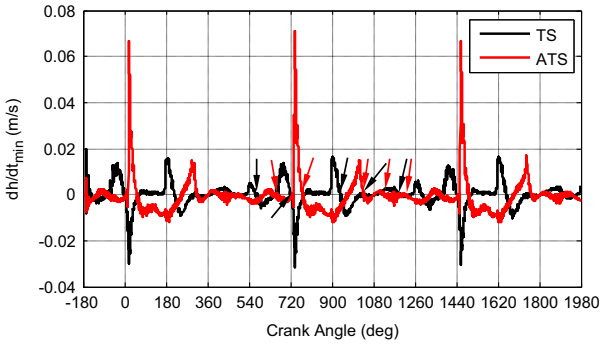

Fig. 8. The film thickness squeeze velocity at 3000 rpm and 27 Nm.

Table 5
Prediction of position (crank angle, degrees) and location of piston slap events for the lubricant squeeze velocity criterion at 3000 rpm and 27 Nm.

	Cycles		
	1st	**2nd**	**3rd**
Crank angle and slap location	−143 (TS) −73 (ATS) 0.6 (TS) 52 (ATS) 214 (TS) 316 (TS - ATS) 406 (ATS) 485 (TS) 497 (ATS)	574 (TS) 647 (ATS) 727 (TS) 773 (ATS) 936 (TS) 1036 (TS – ATS) 1127 (ATS) 1195 (TS) 1216 (ATS)	1290 (TS) 1369 (ATS) 1442 (TS) 1491 (ATS) 1656 (TS) 1770 (TS – ATS) 1833 (ATS) 1911 (TS) 1940 (ATS)

Table 6
Prediction of intervals (crank angle, degrees) and location of piston slap events for the piston-impact angular duration criterion at 3000 rpm and 27 Nm.

	Cycles					
	1st		**2nd**		**3rd**	
	Interval	Location	Interval	Location	Interval	Location
Crank angle and slap location	(−143, −65) (−73, 16) (0.6, 62) (52, 249) (214, 292) (316, 363) (316, 375) (406, 480) (485, 520) (497, 605)	TS ATS TS ATS TS ATS TS ATS TS ATS	(574, 655) (547, 736) (727, 782) (773, 971) (936, 1015) (1036, 1084) (1036, 1092) (1127, 1203) (1195, 1241) (1216, 1322)	TS ATS TS ATS TS ATS TS ATS TS ATS	(1290, 1373) (1369, 1456) (1442, 1502) (1491, 1687) (1656, 1721) (1770, 1805) (1770, 1809) (1833, 1910) (1911, 1963) (1940, –)	TS ATS TS ATS TS ATS TS ATS TS ATS

in the third cycle excludes an ending position (to find the end of it, tribodynamic analysis of the system is required for the fourth cycle).

The validation of the above six theoretical patterns is achieved by identifying the number of theoretical events that match the experimental ones in both crank angle and direction of occurrence (TS or ATS). The measured acceleration on the engine block surface is filtered between 450 and 3500 Hz. In order to identify the major events, 2D Continuous Wavelet Spectra (CWS) are used (Fig. 9) for both TS and ATS accelerations (the events are shown with numbered white circles). Those with higher energy levels are clearly shown over a wider frequency range. The occurrence of these events is noted and then converted into crank angle for comparison purposes with the theoretical predictions. For this particular engine speed/torque combination, three main events are recorded at TS (the third one is spread over a wider time interval and it is noticeably stronger). An explanation about this is discussed later. At ATS, four events are captured for the first two cycles. In the third cycle, the fourth event diminishes slightly and merges with the third one at 2–2.5 kHz.

The noted events in the wavelet spectra (converted into crank angle) are presented in Table 7. The event with the highest energy level is expected to occur in the combustion stroke, where gas and inertia forces are at their highest. In the wavelet

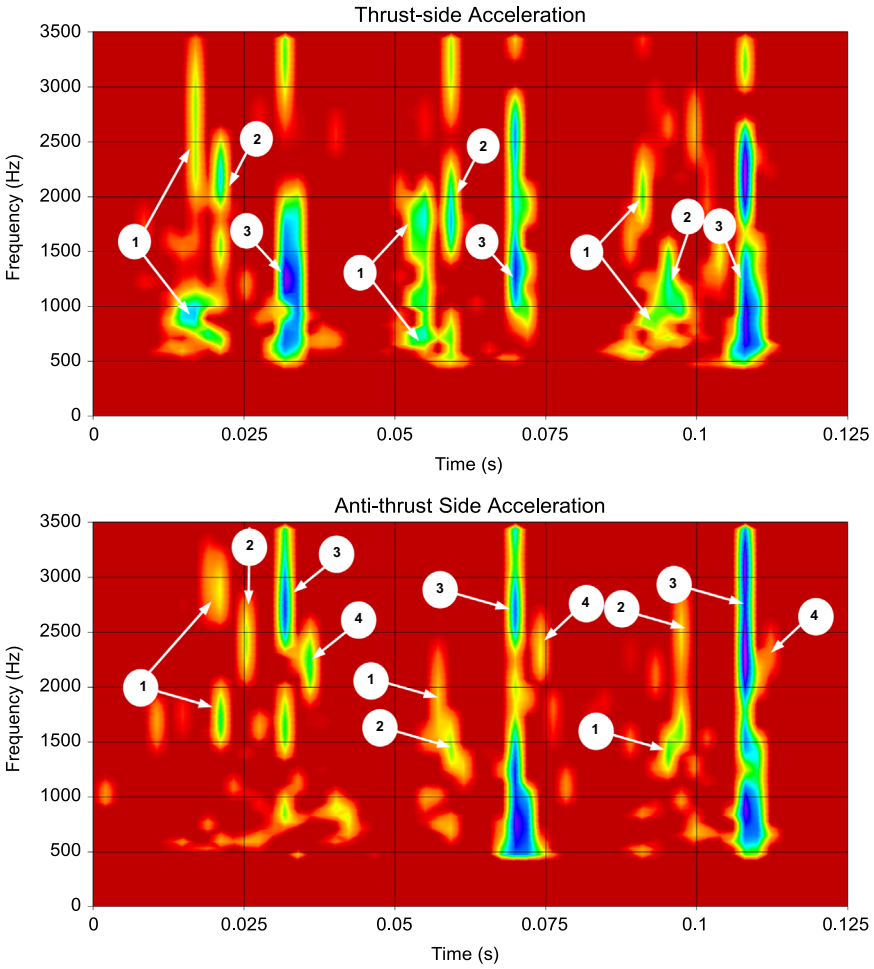

Fig. 9. CWS of the acceleration signals at the TS and ATS (3000 rpm engine speed and 27 Nm input torque).

spectra, it is clear that the event with the highest energy level (number 3 at TS and ATS in Fig. 9) occurs in the intake stroke with long duration and wide frequency range. It appears that another mechanical source contributes to this event. The crank angle and periodicity of the event points to a potential contribution from the exhaust valve closure impact. Based on the engine specifications, the valve opening and closure impacts can coincide with piston slap events at certain crank angles (these are provided in bold in the second column of Table 7).

The experimental events are compared against the theoretical predictions from the six concepts (columns A-F in Table 7): quasi-static lateral force (A), the transient lateral force (B), EHL minimum film thickness (C), the maximum transferred energy (D), the lubricant squeeze velocity (E) and the piston-impact angular duration (F) criteria. The grey cells denote a deviation of about 30° in the predicted positions. These deviations can be due to neglecting the connecting rod effect, as well as other piston assembly components. Overall, in the first cycle, 5 events are predicted at the correct angular position by all concepts, except in column D where the maximum transferred energy concept estimates 6 events. 5 events out of these predictions are estimated in the correct location. This number reduces to 4 for the EHL minimum film thickness concept. The number of the predicted events respectively equals 3, 3, 4, 7, 5 and 7 in the second cycle. In the same sequence, 3, 3, 3, 4, 4 and 6 out of these predicted events agree with the experimental measurements with respect to TS/ATS location. All concepts except E succeed in predicting the correct location in the third cycle. The lubricant squeeze velocity extracts 2 correct locations out of 4 predictions. The quasi-static lateral force, transient lateral force and piston-impact angular duration concepts bring the most successful results (in terms of predicting both correct angular position in the engine cycle and location of impact). Excellent repeatability has been observed when comparing the theoretical predictions to numerous engine cycle intervals in the experimentally obtained signals.

4.2. Engine speed of 3500 rpm and input torque of 40 Nm

Similar analytical and experimental procedures have been applied for 3500 rpm engine speed and 40 Nm input torque. To avoid repetition, commentary is brief but significant differences compared to the previous case are highlighted. The main

Table 7
Experimental crank angle and location for piston slap events at 3000 rpm and 27 Nm versus: (A) quasi-static lateral force; (B) transient lateral force; (C) EHL minimum film thickness occurrence; (D) maximum transferred energy; (E) lubricant squeeze velocity; (F) piston-impact angular duration. [■]: 100% match; [■]: deviation about 30°; [D]: location mismatch; [[ ]]: 100% mismatch.

Cycle	Experimental events	A	B	C	D	E	F
1	**96 (TS)**			■	■		
	196 (TS) – 191 (ATS)	■	■		■	■	■
	300 (TS) – 295 (ATS)	■	■	■	■	■	■
	339 (ATS)	■	■	■	■	■	■
	440 (TS) – 445 (ATS)	■	■	■	■	■	■
	499 (ATS)	■	■	D	D	■	■
2	577 (ATS)				■	D	■
	613 (ATS)			■	D	■	■
	815 (TS)				■		D
	864 (ATS)	■	■		D		■
	920 (TS) – 914 (ATS)			■	■	■	■
	1150 (TS) – 1154 (ATS)	■	■	■	■	■	■
	1228 (ATS)	■	■	D	D	■	■
3	**1495 (TS)**	■	■		■	D	■
	1598 (TS) – 1592(ATS)	■	■		■		■
	1641 (ATS)			■	■	D	■
	1788 (TS)	■	■	■	■	■	■
	1875 (TS) – 1875 (ATS)	■	■	■	■	■	■
total	**Correct in angular position**	12	12	13	18	14	17
	Correct in angular position and location	12	12	10	14	11	16
	Percentage of successfully predicted events (direction and occurrence)	**100**	**100**	**77**	**78**	**79**	**94.1**

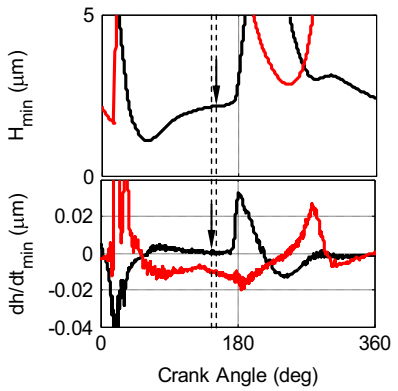

Fig. 10. The incipient theoretical event due to the increase in engine speed and load.

changes are observed in the criteria that are based on piston transient tribodynamics. As the engine speed increases, piston inertia contributes more and film thickness squeezes further. An incipient minimum film thickness is observed about 30–40° before BDC in the combustion stroke. This event is shown in the H_{min} graph of Fig. 10. A similar event appearance is

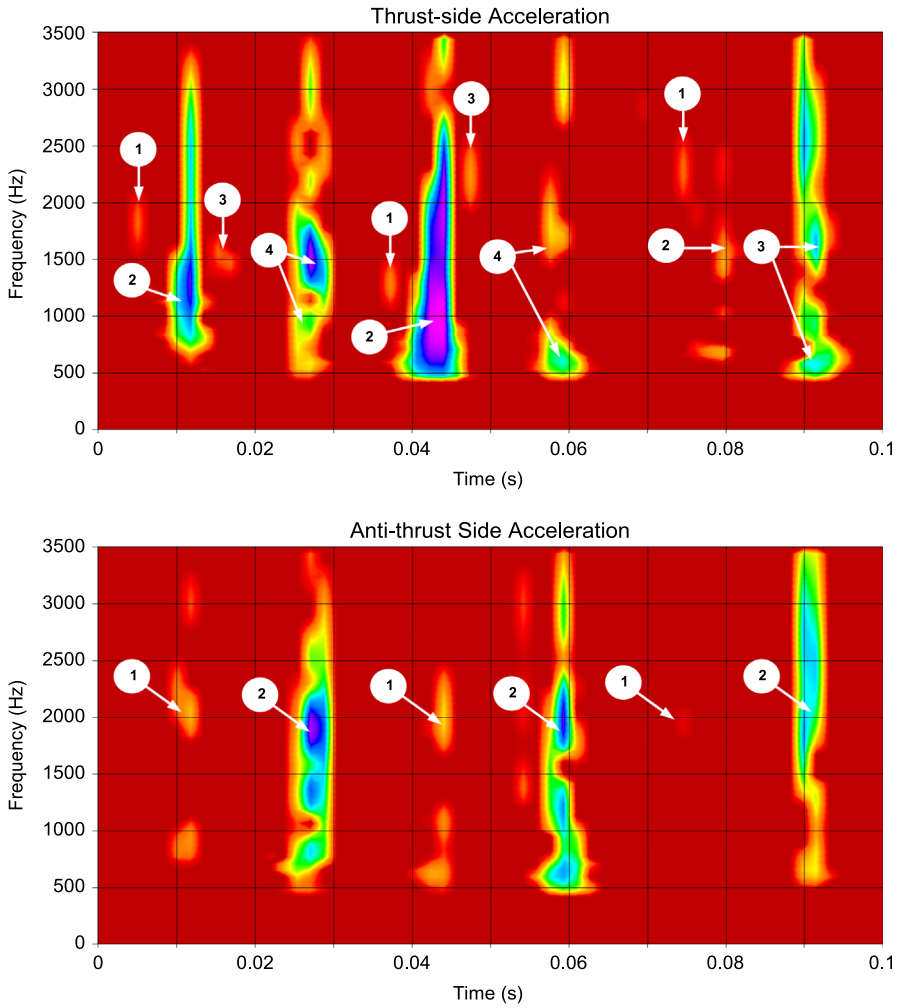

Fig. 11. CWS of the acceleration signals at the TS and ATS (3500 rpm engine speed and 40 Nm input torque).

investigated in the lubricant squeeze velocity. At about the same position, oil film squeezes for a very short time and then continues to recede. The combination of these two events results in the introduction of a small piston-impact angular duration. These events are depicted by black arrows and dotted lines in Fig. 10.

CWS are investigated for the measured surface accelerations in Fig. 11. In the TS spectrum, four events are present in each engine cycle. The two larger events are easily distinguishable. In the proximity of the first one, two smaller events are observed. The first three events diminish in the beginning of the third cycle but their trace can still be seen. The number of consistently repeatable events reduces to two at ATS. In the last cycle, the first event does not have as high energy as the others. In both directions, the significant event in the intake stroke is stronger than the other events. As already mentioned, this behaviour can be again correlated to exhaust valve closure impact. The crank angles where valve impact events coincide with piston slap events are shown in bold in the second column of Table 8.

The time of experimental events is again converted into crank angle. The measured crank angle values are given in Table 8 along with the comparison with the theoretical predictions. The first event happens at -77°. This contribution is captured by the EHL minimum film thickness occurrence and squeeze velocity concepts. In the first cycle, the rest of the events are correctly estimated by the six criteria with respect to TS/ATS location. At 133° crank angle, the cells with asterisks correspond to the incipient events described earlier. For three consecutive cycles, the quasi-static lateral force and transient lateral force concepts identify 3, 4 and 3 matches based on position. 3, 3 and 2 out of these events are in accordance with the experiment in terms of direction. The EHL minimum film thickness criterion identifies 4, 5 and 3 events in each cycle. All these succeed direction-wise. The maximum energy concept identifies 3 angular positions with the correct location in each cycle. The lubricant squeeze velocity fails to identify the right location at the beginning of the first and second cycles; besides that, it is capable of recording all the events. The only discrepancy in the piston-impact angular duration criterion is observed in the first event of the second cycle. In total, techniques based on transient film thickness describe better the piston-cylinder interactions. The most successful criterion is the EHL minimum film thickness occurrence.

Table 8
Experimental crank angle and location for piston slap events at 3500 rpm and 40 Nm versus: (A) quasi-static lateral force; (B) transient lateral force; (C) EHL minimum film thickness occurrence; (D) maximum transferred energy; (E) lubricant squeeze velocity; (F) piston-impact angular duration. [ ]: 100% match; [ ]: deviation about 30°; [D]: location mismatch; [ ]: 100% mismatch.

Cycle	Experimental events	A	B	C	D	E	F
1	**-77 (TS)**					D	
	33 (TS) – 36 (ATS)						
	133 (TS)			*		*	*
	439-470 (TS – ATS)						
2	**675 (TS)**				D	D	D
	763 (TS) – 770 (ATS)						
	867 (TS)	D	D	*		*	*
	1043 (ATS)						
	1135-1170 (TS – ATS)						
3	1470 (TS) – 1468(ATS)						
	1597(TS)	D	D	*		*	*
	1860-1897 (TS – ATS)						
total	**Correct in angular position**	10	10	12	10	12	12
	Also correct in angular position and location	8	8	12	9	10	11
	Percentage of successfully predicted events (direction and occurrence)	**80**	**80**	**100**	**90**	**83**	**92**

4.3. Engine speed of 4250 rpm and input torque of 42 Nm

The analysis of piston's secondary motion is presented for the quasi-static lateral force and transient lateral force in Fig. 12. Comparison between Figs. 12 and 5 reveals that the quasi-static lateral force noticeably deviates from the transient lateral force graph. The former concept fails to follow piston slap events in most parts of the engine cycle. Using piston tribodynamics, two events are added to the lateral force direction predictions. These two can be pinpointed in the compression stroke and at about 70–90° before the TDC. At these angular positions, lateral force changes direction for a short period of time. The incipient minimum film thickness described in the previous engine condition is also present in the current engine speed.

The CWS are given in Fig. 13 for the measured surface accelerations. As can be seen, some events are merged. The first cycle is between 0 and 0.03 s. Two large events are shown around 0.01 s and 0.025 s. A smaller contribution is clearly observed at about 0.005 s. The second cycle starts at about 0.03 s and ends around 0.055 s. The beginning of the cycle is unclear because events are slightly merged. Four events are available in the 0.03–0.045 s time interval. The last major event appears at about 0.05 s. A similar merging of events exists between 0.055 and 0.065 s in the third cycle. Unlike the TS spectrum, events are clearly highlighted at ATS with 4 events occurring in the first cycle. The number of events reduces to 2 and 3 in the next two cycles. The event that happens after 0.06 s is not as strong as the other contributions; however, it is distributed over a wide frequency range.

The crank angle position of piston events identified through the CWS is shown in Table 9. The events highlighted in bold may correspond to the valve opening and closure, as well as piston events. The measured and predicted events are compared using the six criteria in the same table. The cells with asterisks again correspond to the incipient minimum film thickness occurrence mentioned before. In the first cycle, the number of predicted events by the six concepts is 2, 4, 4, 3, 4 and 4, respectively. These events are all correct in direction, except those for the EHL minimum film thickness occurrence and squeeze velocity concepts. 3 out of 4 predictions are in accordance with the experiment in the latter criteria. In the second engine cycle, the only concept that thoroughly estimates the piston events is the EHL minimum film thickness. Other concepts fail to follow 1 or 2 events out of the predicted ones in terms of direction. The total number of correct events is 2, 3, 3, 3, 3 and 4 out of 3, 5, 3, 5, 4 and 5 estimations. The pattern of correct events changes to 1, 3, 5, 5, 3 and 5 in the third cycle. Only the locations in the EHL minimum film thickness occurrence completely match the experimental ones. In total, the

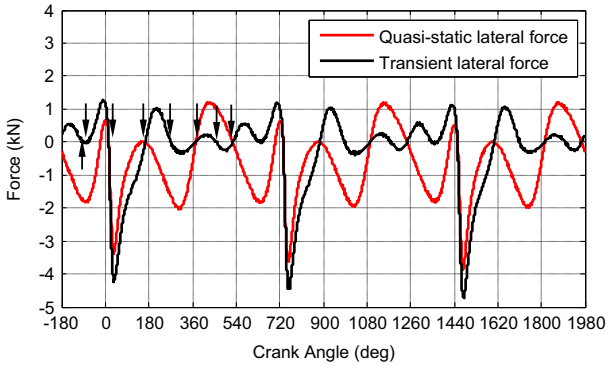

Fig. 12. Lateral forces for quasi-static and transient criteria at 4250 rpm and 42 Nm.

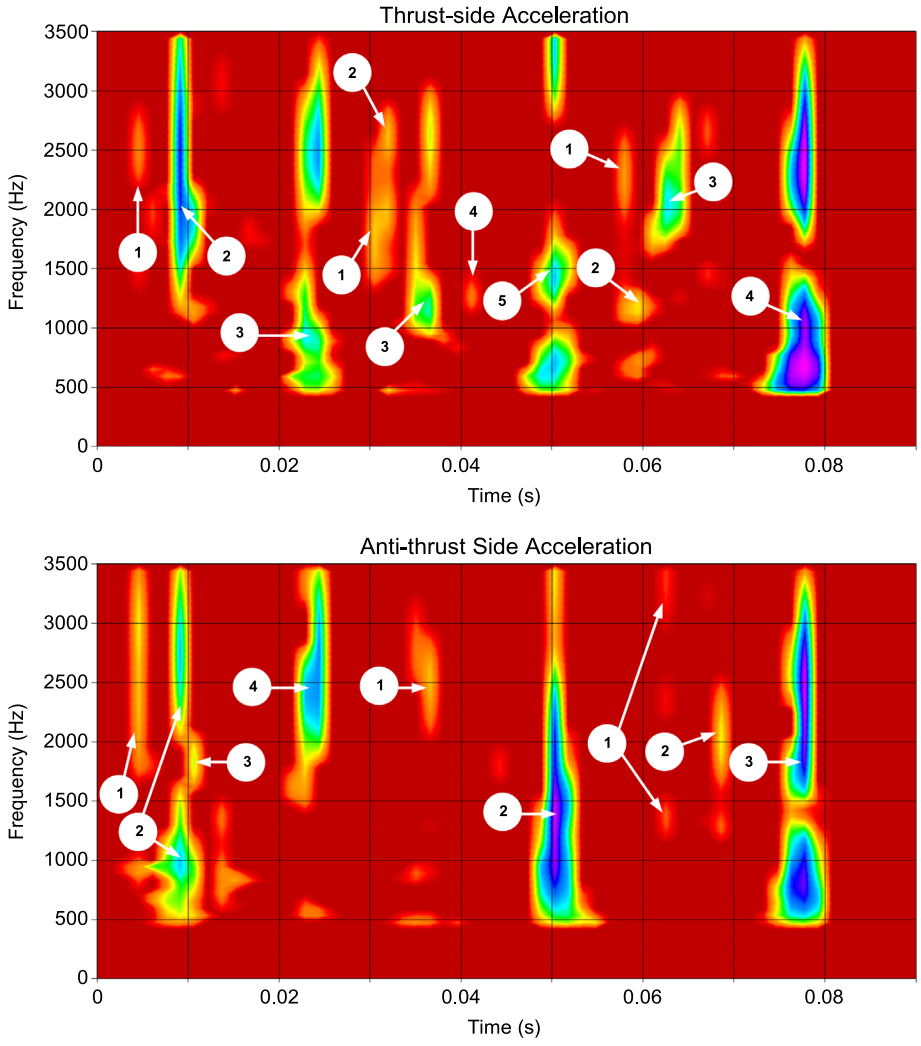

Fig. 13. CWS of the acceleration signals at the TS and ATS (4250 rpm engine speed and 42 Nm input torque).

methods based on film variations are more accurate as the engine speed increases. Amongst these techniques, the EHL minimum film thickness occurrence and the lubricant squeeze velocity are the most successful.

The overall performance (combined outcome for all three different engine speed/load combinations) of each identification method is given in Fig. 14 and comparison is established herein. The 45 experimentally measured events are used as a reference to assess the performance of the theoretical identification methods. Initially, the total number of events predicted

Table 9
Experimental crank angle and direction for piston slap events at 4250 rpm and 42 Nm versus: (A) quasi-static lateral force; (B) transient lateral force; (C) EHL minimum film thickness occurrence; (D) maximum transferred energy; (E) lubricant squeeze velocity; (F) piston-impact angular duration. [■]: 100% match; [▒]: deviation about 30°; [D]: location mismatch; [[ ]]: 100% mismatch.

Cycle	Experimental events	A	B	C	D	E	F
1	**-65 (TS – ATS)**		■	▒		■	■
	32(TS – ATS)	■	■	■	■	▒	■
	164 (ATS)	■	■	D	▒	D	■
	423-476(TS – ATS)		■	■	■	■	■
2	**635 (TS)**		■	■	▒		■
	665 (TS)	D	D		D	D	D
	766(TS – ATS)	▒	▒	■	■	▒	■
	910 (TS)	■	D	*	D	*	*
	1170(TS – ATS)		■	■	■	■	■
3	**1364 (TS)**		■	■	■		■
	1397 (TS)	D	D		D	D	D
	1466(TS) – 1462(ATS)	■	■	■	■	■	■
	1594 (TS)	D		*		*	*
	1647 (ATS)			▒		D	■
	1874-1904(TS – ATS)		■	■	■	■	■
total	**Correct in angular position**	8	13	13	14	13	15
	Also correct in angular position and location	5	10	12	11	9	13
	Percentage of successfully predicted events (direction and occurrence)	**63**	**77**	**92**	**79**	**69**	**87**

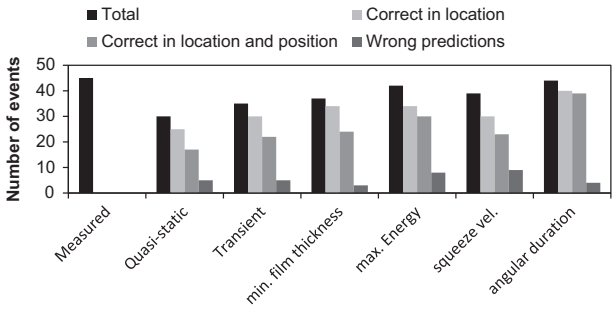

Fig. 14. Comparison between the different identification methods of piston-impact events.

by each method is shown, regardless of the accuracy in predictions. The greatest number of events is captured (in descending order) by the following methods: angular duration, maximum energy, film squeeze velocity, minimum film thickness, transient lateral force and quasi-static lateral force. The results are further refined considering the event location (i.e. TS and ATS). The angular duration method predicts 40 events in the correct location. The maximum energy and the minimum film thickness methods equally share the second place in predicting the correct number of events followed by the film squeeze velocity and transient lateral force techniques. As discussed earlier, some theoretical predictions deviate slightly (about 30°) from the actual measured event; therefore, the number of predicted events has been updated using both location and angular position, as shown in the figure. In this case the angular duration method is the most accurate approach. The number of mismatched event (in terms of location) is also depicted in the figure. The minimum film thickness method accounts for the least number of wrongly predicted events. The angular duration and maximum energy methods consistently and accurately identify the maximum number of correct events and are commended as the best identification

techniques in this work; the latter suggests the exact position of piston impact events, while the former provides an estimate for the angular interval of each single event.

5. Conclusions

In this paper, six concepts have been used to study potential piston slap events in internal combustion engines. In the available literature, identification methods for piston-liner impacts have been proposed based on the quasi-static contribution of forces in the lateral direction of piston motion, on sign change of the transient lateral force and on occurrence of the minimum film thickness. Three additional concepts were introduced in this study, which are the maximum transferred energy, the lubricant squeeze velocity and the piston-impact angular duration. A single cylinder petrol engine experimental rig was employed to validate the concepts studied. It is shown that the quasi-static and transient lateral force concepts are successful in the prediction of angular position and location of events at lower engine speeds and loads. At higher engine speed/load combinations (with larger inertia contributions), the transient mechanism of the minimum film thickness occurrence proves to be a more successful criterion. The piston-impact angular duration and maximum energy methods are those techniques sustaining their effectiveness in estimating impact events through all the engine tests. The angular duration method suggests an interval for the occurrence of each event, while the maximum energy method points out the accurate event position. It is also shown that the number of events increases in theory as the engine speed increases. The examined concepts reveal that transient tribodynamic analysis is a very useful technique to identify the number of piston slap events, as well as their severity as a result of the engine speed/load conditions (particularly at higher speeds necessitating capture of faster impact events). As future work, the accuracy of the examined methods may be investigated in different engine configurations (higher number of cylinders) and various speed/load ranges. In addition, the effects of connecting rod inertia and friction force can be added in the systems modelled.

Acknowledgement

The authors wish to express their gratitude to the EPSRC for the financial support extended to the Encyclopaedic Programme Grant (EP/G012334/1), under which this research was carried out. Thanks are also due to the consortium of industrial partners of the Encyclopaedic project, particularly to Capricorn Automotive.

References

[1] X. Meng, Y. Xie, A new numerical analysis for piston skirt-liner system lubrication considering the effects of connecting rod inertia, Tribol. Int. 47 (2011) 235–243.
[2] R. Edara, Reciprocating engine piston secondary motion – literature review, SAE International 2008-01-1045, 2008.
[3] F. Noor Balia, M. Ridha, A. AB Wahab, Investigation into piston-slap force under friction and connecting rod effects of diesel engine, in: Proceeding of the International Conference on Advanced Science, Engineering And Information Technology, 2011.
[4] Z. Geng, J. Chen, Investigation into piston-slap-induced vibration for engine condition simulation and monitoring, J. Sound Vib. 282 (3) (2005) 735–751.
[5] E.E. Ungar, D. Ross, Vibrations and noise due to piston-slap in reciprocating machinery, J. Sound Vib. 2 (2) (1965) 132–146.
[6] S. Balakrishnan, H. Rahnejat, Isothermal transient analysis of piston skirt-to-cylinder wall contacts under combined axial, lateral and tilting motion, J. Phys. D 38 (5) (2005) 787.
[7] J. CHO, Effects of skirt profiles on the piston secondary movements by the lubrication behaviors, Int. J. Automot. Technol. 5 (1) (2004) 23–31.
[8] O. Reynolds, On the theory of lubrication and its application to mr. beauchamp tower's experiments, including an experimental determination of the viscosity of olive oil, Proc. R. Soc. Lond. 40 (242–245) (1886) 191–203.
[9] V. D' Agostino, D. Guida, A. Ruggiero, C. Russo, Optimized EHL piston dynamics computer code, in: Proceedings of the 5th International Tribology Conference, AITC-AIT, 2006.
[10] M. Perera, S. Theodossiades, H. Rahnejat, Elasto-multi-body dynamics of internal combustion engines with tribological conjunctions, Proc. Inst. Mech. Eng., Part K: J. Multi-body Dyn. 224 (3) (2010) 261–277.
[11] M. Perera, S. Theodossiades, H. Rahnejat, A multi-physics multi-scale approach in engine design analysis, Proc. Inst. Mech. Eng., Part K: J. Multi-body Dyn. 221 (3) (2007) 335–348.
[12] de Luca, Julio Cesar, S.N.Y. GERGES, Piston Slap Excitation: Literature Review, 1996.
[13] M. Chiollaz, B. Favre, Engine noise characterisation with Wigner-Ville time-frequency analysis, Mech. Syst. Signal Process. 7 (5) (1993) 375–400.
[14] J. Richmond, D. Parker, The quantification and reduction of piston slap noise, Proc. Inst. Mech. Eng. Pt. D: J.Automobile Eng 201 (4) (1987) 235–244.
[15] L. Pruvost, Q. Leclere, E. Parizet, Diesel engine combustion and mechanical noise separation using an improved spectrofilter, Mech. Syst. Signal Process. 23 (2009) 2072–2087.
[16] J. Antoni, Blind separation of vibration components: Principles and demonstrations, Mech. Syst. Signal Process. 19 (2005) 1166–1180.
[17] X. Liu, R.B. Randall, Blind source separation of internal combustion engine piston slap from other measured vibration signals, Mech. Syst. Signal Process. 19 (2005) 1196–1208.
[18] M.E. Badaoui, J. Daniere, F. Guillet, C. Servière, Separation of combustion noise and piston-slap in diesel engine—Part I: separation of combustion noise and piston-slap in diesel engine by cyclic wiener filtering, Mech. Syst. Signal Process. 19 (6) (2005) 1209–1217.
[19] C. Servière, J. Lacoume, M. El Badaoui, Separation of combustion noise and piston-slap in diesel engine—Part II: Separation of combustion noise and piston-slap using blind source separation methods, Mech. Syst. Signal Process. 19 (6) (2005) 1218–1229.
[20] J. Chen, R. Randall, Vibration signal processing of piston slap and bearing knock in IC engines, Surveillance 6 (2011).
[21] B. Littlefair, M. De La Cruz, R. Mills, S. Theodossiades, et al., Lubrication of a flexible piston skirt conjunction subjected to thermo-elastic deformation: a combined numerical and experimental investigation, Proc. Inst. Mech. Eng. Part J (2013).
[22] Sashi Balakrishnan, Transient Elastohydrodynamic Analysis of Piston Skirt Lubricated Contact Under Combined Axial, Lateral and Tilting Motion (Doctoral), Loughborough University, 2002.
[23] D. Dowson, G. Higginson, A numerical solution to the elasto-hydrodynamic problem, J. Mech. Eng. Sci. 1 (1) (1959) 6–15.

[24] C. Roelands, Correlational Aspects of the Viscosity-Temperature-Pressure Relationship of Lubricating Oils (Ph.D.), Technical University Delft, 1966.
[25] B. Littlefair, M. De la Cruz, R. Mills, S. Theodossiades, et al., Transient tribo-dynamics of thermo-elastic compliant high performance piston skirts. Tribol. Lett. (2013) 1–20, http://dx.doi.org/10.1007/s11249-013-0243-6.
[26] K. Ohta, Y. Irie, K. Yamamoto, H. Ishikawa, Piston slap induced noise and vibration of internal combustion engines (1st report, theoretical analysis and simulation). SAE Paper 870990, 1987.
[27] K. Nakashima, Y. Yajima, K. Suzuki, Approach to minimization of piston slap force for noise reduction–investigation of piston slap force by numerical simulation, JSAE Rev. 20 (2) (1999) 211–216.